International Journal of Recent Technology and Engineering (IJRTE)
ISSN: 2277-3878 (Online), Volume-12 Issue-1, May 2023

# Experimentation of MPPT Control Driving a Buck Converter with PV Module Disturbances and Variable Load in a Nanogrid

**Sandaniaina Sedinirina Andriamihaingo Ranaivoson, Nicolas Saincy, Eric Jean Roy Sambatra, Todizara Andrianajaina, Nirinason Jean Razafinjaka**

***Abstract*****:** ***The objective of this paper is to perform a laboratory test on the performance of MPPT control in a nanogrid. The components used for tests are described, namely (i) a PV module SPP031001200 manufactured by Victron energy, a prototype of a synchronous buck converter controlled by Arduino Atmel ATmega V-2560, and a DC electronic load programmable 72-13210 manufactured by TENMA$^{TM}$. Among several MPPT controls, the choice falls on the methods Perturb and Observe "P&O" and Increment of the conductance "INC" which are more widely used than others. Laboratory tests with different PV module conditions and variable output voltage were performed. In full sunlight, the input power of the buck converter gives a better result with the INC method compared to the P&O method. For a PV module exposed to horizontal or vertical total shading, INC method gives a small advantage compared to the P&O method, which can be beneficial for a long time. Compared to the P&O method, INC method always gives better results due to its more complex algorithm. Due to the lack of measuring instruments, the different tests were performed without considering irradiance and temperature.***

***Keywords*****:** ***Buck Converter, DC Electronic Load, MPPT, Solar Home System.***

## I. INTRODUCTION

In Madagascar, electricity needs are today served by two radically distinct approaches which are the construction and operation of traditional power grids on the one hand; and the distribution of individual off-grid electric systems on the other hand [1], [2].

Traditional power grids can prevail of a significant impact on local economic and social development in the zones where it is deployed, but they failed for several years to answer the challenge of access to electricity. Its distribution rhythm is indeed today lower than the population growth rate, because of the colossal investment costs, long implementation times, tariff offers poorly adapted to the local context, development potential limited to relatively dense demand areas in very largely rural countries, etc. [1]-[4].

On the other hand, the diffusion of Solar Home Systems has spread at a spectacular speed over the last decade and, by offering a simple, fast, and affordable response to the basic demands of off-grid populations, has already made it possible to rapidly improve the living conditions of many people. However, the level of service is limited to domestic needs and not flexible, the limited lifetime of the equipment implies a high long-term cost, but above all a renunciation of infrastructure construction, etc. [1], [5], [6].

In this context, the weakness of the current development of electrical infrastructures in Madagascar, with renewable energies, the development of new technologies of electrical conversion, and smart grids offer a formidable opportunity to develop 21st-century electrical infrastructures more rapidly [1], [7].

The ambition of the Lateral Electrification model is to emancipate the constraints of the two current electrification models to bring out a third voice capable of reconciling the short-term and long-term challenges of the electricity sector in Madagascar by proposing an efficient solution and ultra-replicable based on i) the distribution of collective autonomous solar DC power system connecting 4 to 6 neighboring users (called "nanogrids") to quickly answer the energy needs of households and ii) their progressive interconnection to participate in the construction of the bottom-up of 21st-century electrical infrastructures (decarbonized, decentralized and digitized), capable of meeting the growing productive energy needs of rural areas [1], [8].

The technologies allowing the implementation of the first stage of this model (i.e., "nanogrids") have already been developed and tested by the company Nanoé. DC power distribution was chosen for reasons of energy efficiency, simplicity, and cost.

**Manuscript received on 27 April 2023 | Revised Manuscript received on 08 May 2023 | Manuscript Accepted on 15 May 2023 | Manuscript published on 30 May 2023.**
*Correspondence Author(s)
**Sandaniaina Sedinirina Andriamihaingo Ranaivoson***, Nanoé Company - Decentralized Electrification, Ambanja, Madagascar. Email: sanda.ranaivo@gmail.com, ORCID ID: https://orcid.org/0000-0002-5777-8089
**Nicolas Saincy**, Nanoé Company - Decentralized Electrification, Madagascar. Email: nicolas.saincy@nanoe.net
**Eric Jean Roy Sambatra**, School of Industrial Engineering, Higher Institute of Technology, Antsiranana, Madagascar. Email: ericsambatra@gmail.com
**Todizara Andrianajaina**, Department of Electrical and Electronic Engineering, Higher Polytechnic School, Antsiranana, Madagascar. Email: todizara.andrianajaina@gmail.com
**Nirinason Jean Razafinjaka**, Department of Electrical and Electronic Engineering, Higher Polytechnic School, Antsiranana, Madagascar. Email: razafinjaka@yahoo.fr

For the second stage of this process, research works are carried out to study the feasibility of interconnecting several nano-grids with each other within DC balancing microgrids of village scale [1], [8]-[10]. Among which, simulations on the Matlab / Simulink © environment have
been performed to produce the maximum power in an electrical nanogrid using the Maximum Power Point Tracking "MPPT" technique with the commands Perturb and Observe "P&O" and Increment of the Conductance "INC" due to their ease of implementation compared to other MPPT controls [10].

This paper proposes a design and prototyping of a buck converter driven by the "P&O" and "INC" controls using a microcontroller. Laboratory tests are performed using a PV module connected directly to a DC electronic load as a reference.

This article is divided into the following sections: Section 2 talks about the equipment used on the test bench with details on the prototype of the buck converter and the choice of MPPT controls. Then, in section 3, laboratory experiments under the influence of disturbances at the PV module and the output of the buck converter followed by discussions take place. Some conclusions are drawn in section 4.

## II. MATERIALS AND METHODS

First, in Fig. 1, a PV module is connected directly to a DC electronic load to have its power curve for a voltage from 0 to Voc.

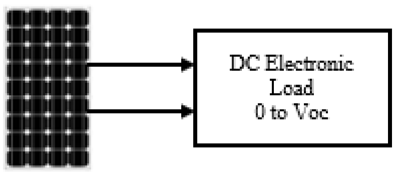


**Fig. 1: PV module directly connected to a DC electronic load**

In Fig. 2., a buck converter ensures adaptation between the PV module and the DC electronic load.
Buck converter is driven by an MPPT control that generates a duty cycle using the voltage and current measurements provided by the PV module. The output voltage of the DC electronic load varies from 10 to 15V to have the same operation as a 12V battery in charging mode.

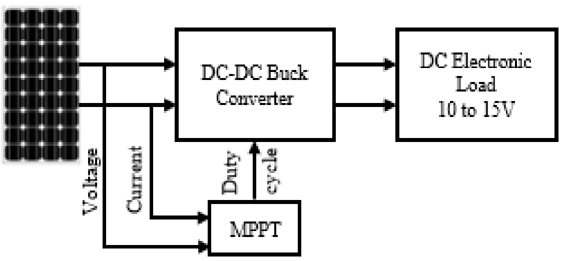


**Fig. 2: Use of a buck converter driven by a MPPT control**

### A. PV module

A PV module is formed by the association of several PV cells, which can be considered as an ideal source of current providing a current $I_{ph}$ proportional to the irradiance and the temperature [10], [11].

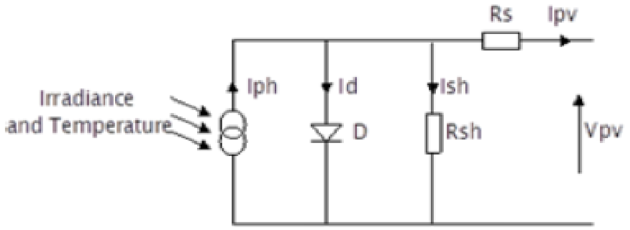


**Fig. 3: Single-diode model of a photovoltaic cell**

In Fig. 3, the equations corresponding to a model with a diode of a photovoltaic cell are summarized by:

$$I_{pv} = I_{ph} - I_d - I_{sh}, \tag{1}$$

The Photocurrent is expressed as a function of irradiance and temperature:

$$I_{ph} = \frac{\phi}{\phi_{ref}}\left[I_{cc} + \mu_{Icc}\left(T - T_{ref}\right)\right], \tag{2}$$

It is assumed that the diode current is related to the temperature according to the expression:

$$I_d = I_{sat} * \left[\exp\left(\frac{V_{pv} + R_s I_{pv}}{nV_T}\right) - 1\right], \tag{3}$$

And the shunt current through the shunt resistor is equal to:

$$I_{sh} = \frac{V_{pv} + R_s I_{pv}}{R_{sh}}. \tag{4}$$

With $V_{pv}$ and $I_{pv}$ represent the voltage and current of the PV cell, $\phi$ and $\phi_{ref}$ are real and reference irradiances $[W/m^2]$ ; $T$ and $T_{ref}$ are effective and reference temperatures $[K]$ ; is the temperature coefficient of the short-circuit current; $I_{sat}$ is the saturation current [A]; is the ideality factor of the junction $(1 < n < 3)$ et and the thermal voltage of the diode [V].

Table- I summarizes the characteristics of the PV module used in this paper.

**Table- I: PV Module Characteristic**

| | |
|---|---|
| Mark | Victron Energy |
| Model | SPP031001200 |
| Power at MPP (Pmpp) | 100 W |
| Voltage at MPP (Vmpp) | 17,2 V |
| Current at MPP (Impp) | 5,8 A |
| Open circuit voltage (Voc) | 21,8 V |
| Short circuit current (Isc) | 6,18 A |

Retrieval Number: 100.1/ijrte.A76260512123
DOI: 10.35940/ijrte.A7626.0512123
Journal Website: www.ijrte.org



Published By:
Blue Eyes Intelligence Engineering
and Sciences Publication (BEIESP)

### B. DC-DC converter

#### 1. Buck converter

The DC-DC converter used is a synchronous buck converter, because a MOSFET S2 is used in place of a freewheeling diode [12].

The operation of Fig. 4 can be divided into two phases, depending on the state of switches S1 and S2 [13]:

- switch S1 is closed (S2 open): the current supplied by the PV gradually charges inductance L during $t1 \in \overline{0, dT}$, and the voltage at the output of the converter is defined by:

$$V_{out} = V_{in} - V_L, \tag{5}$$

- switch S1 is open (S2 closed): the current flowing through the inductor decreases during $t2 \in \overline{dT, T}$, and this time it opposes this reduction in current:

$$V_L = -V_{out}, \tag{6}$$

- The duty cycle $d$ is defined by the ratio between the conduction time of S1 and the switching period T:

$$d = \frac{t1}{T}, \tag{7}$$

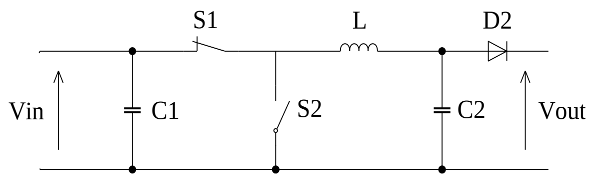


**Fig. 4: Non-isolated synchronous buck converter**

Summary in Table 2, the prototype of the buck converter uses resistors divider bridges to measure input and output voltage, shunt resistor to measure input current, MOSFETs as switches, IR 2104 as a bootstrap circuit to drive S1 and S2 switches, and Arduino MEGA 2560 as a microcontroller.

**Table- II: Synchronous buck converter characteristic**

| | |
|---|---|
| Input voltage Vin | 10 – 30 V DC |
| Output voltage Vout | 10 – 20 V DC |
| Input current | 15 A maximum |
| C1 and C2 capacitor | 470 uF |
| Inductor L | 100 uH |
| S1 and S2 switches | MOSFET IPP12CN10L |
| Blocking diode D2 | 10A02 |
| MOSFET driver | IR 2104 |
| Switching frequency of S1 and S2 | 31,25 kHz |
| Microcontroller | Arduino MEGA 2560 |

#### 2. Microcontroller

The microcontroller on the buck converter is an Atmel ATmega V-2560 Arduino board. A voltage of 5V DC powers this 8-bit microcontroller.

It is made up of many peripherals, of which the ones we use are:

- Analog acquisition module (ADC): to measure the value of the voltages at the terminals of the dividing bridges and the current sensor.

- PWM module (with a frequency of 31.25 kHz): to control the MOSFETS using the duty cycle.

#### 3. Current and voltage sensor

**Voltage measurement**

A voltage divider bridge adapts the voltage level of the PV module to be readable by the ADC of the arduino (the value range of the ADC of the arduino is 0 to 5V DC).

The resistor value pair formed by R1 (51 kOhm) and R2 (10 kOhm) makes it possible to measure a voltage up to 30V DC, has been implemented at the input of the buck converter. The maximum open circuit voltage of the PV module is 21,8 V for an STC condition.

At the output of the buck converter, the pair of resistors R1 (30 kOhm) and R2 (10 kOhm) makes it possible to measure a voltage up to 20V DC.

**Current measurement**

The current measurement uses a 15 mOhm shunt resistor and a differential amplifier at these terminals (INA181A1). With these components, the gain of the current sensor (G = 20 V/V) makes it possible to measure a maximum current of 16 A. The maximum short-circuit current of the PV module is 6.12 A for an STC condition.

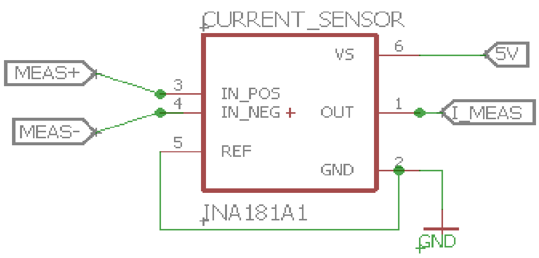


**Fig. 5: Current sensor INA181A1**

Fig. 6, supplemented by Table 2, illustrates the converter used in this article :

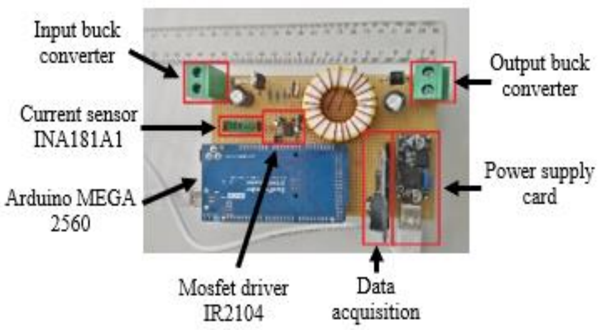


**Fig. 6: Prototype used grouping the control and power part**

### C. MPPT strategy control

MPPT is a command which consists in extracting the maximum power in a non-linear source, by playing on the variation of the duty cycle in a DC-DC converter [14]-[16]. There exist many MPPT algorithms such as constant voltage tracking, P&O method, INC method, genetic algorithm, fuzzy logic control method, neural network method, sliding mode control method, predictive control technique, quadratic maximization method, and so on [14], [15].

In this paper, we will compare the performance of the Perturb and Observe and Conductance Increment methods which are more widely used than others [10], [14], [15].

**1. P&O**

The P&O method consists of varying the voltage $V_{pv}$ and observing the impact on the output power of the PV module [17], [18]. At each cycle (Fig. 7), $V_{pv}$ and $I_{pv}$ are measured to calculate $P_{pv}(k)$, which will be compared to the previous power value $P_{pv}(k-1)$.

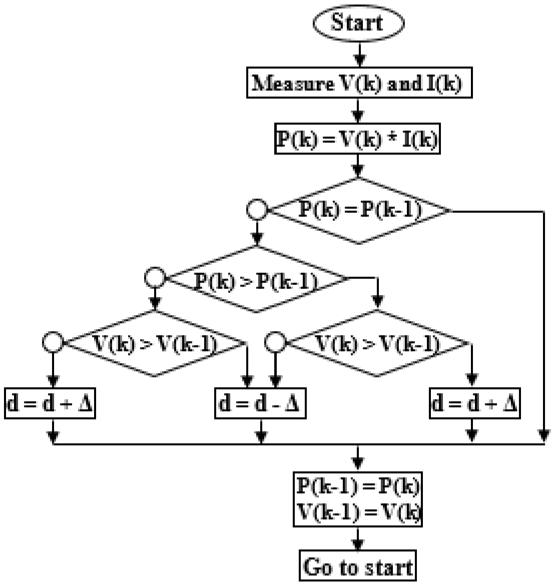


**Fig. 7: Flow chart of P&O method**

**2. INC**

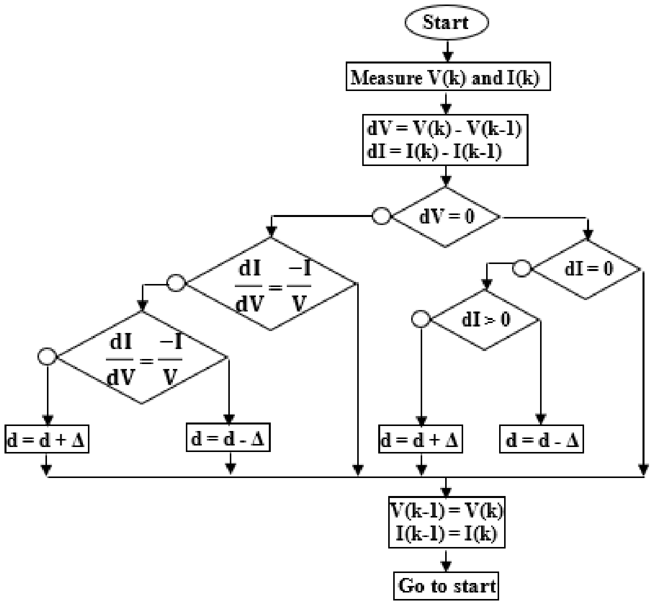


**Fig. 8: Incremental conductance algorithm flow chart**

This method is based on the calculation of the ratio of the derivatives of power and voltage $\frac{dP}{dV}$ to reach the point of maximum power [17], [18].

Knowing that the derivative of the product compared to the tension gives the following relation:

$$\frac{dP}{dV} = \frac{d(V*I)}{dV} = I + V\frac{dI}{dV}, \quad (8)$$

The required incremental changes dV and dI are obtained by comparing the most recent measured values for V and I to those measured during the previous cycle (Fig. 8).

**D. DC load**

A programmable DC electronic load type 72-13210, manufactured by TENMATM, was used, firstly to measure the power supplied by the PV module in direct mode (for a voltage ranging from 0 to $V_{OC}$), then secondly to ensure the role of a battery to the output of the DC converter (for a voltage ranging from 10 to 15).

**E. Focus time**

Every 5 seconds, the voltage of the DC electronic load at the output of the buck converter varies with a step of 0.5V


**Fig. 9: Bench test**

## III. RESULTS AND DISCUSSION

**A. Results**

**1. In full sunlight**

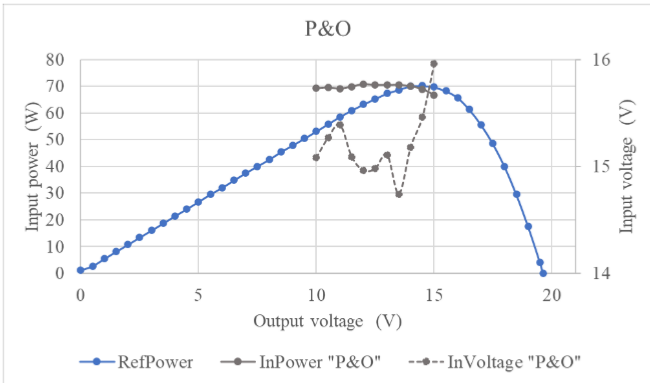


**Fig. 10: Input power and voltage with P&O**

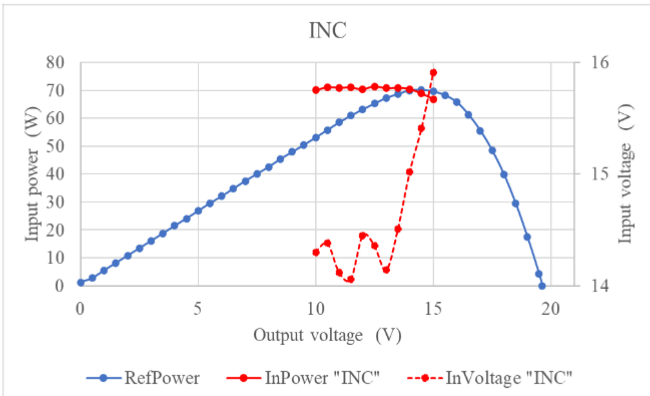


**Fig. 11: Input power and voltage with INC**

*Retrieval Number: 100.1/ijrte.A76260512123*
*DOI: 10.35940/ijrte.A7626.0512123*
*Journal Website: www.ijrte.org*



*Published By:*
*Blue Eyes Intelligence Engineering and Sciences Publication (BEIESP)*

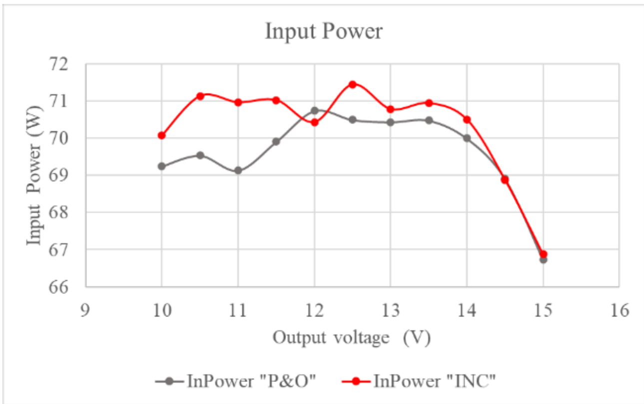


**Fig. 12: Input power with P&O and INC**

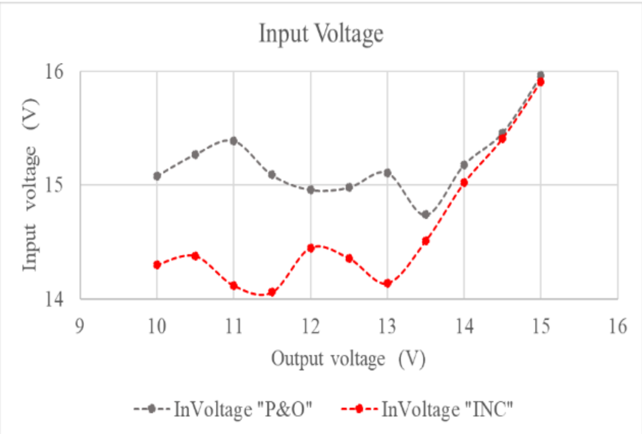


**Fig. 13: Input voltage with P&O and INC**

**2. Total horizontal shading**

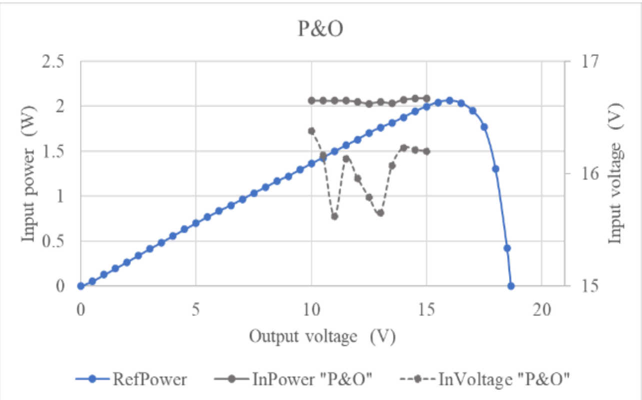


**Fig. 14: Input power and voltage with P&O**

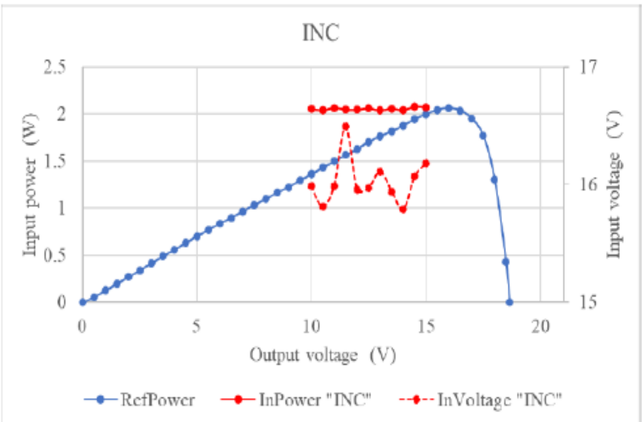


**Fig. 15: Input power and voltage with INC**

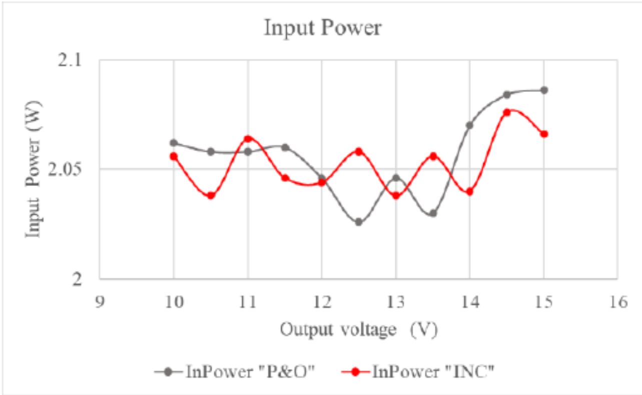


**Fig. 16: Input power with P&O and INC**

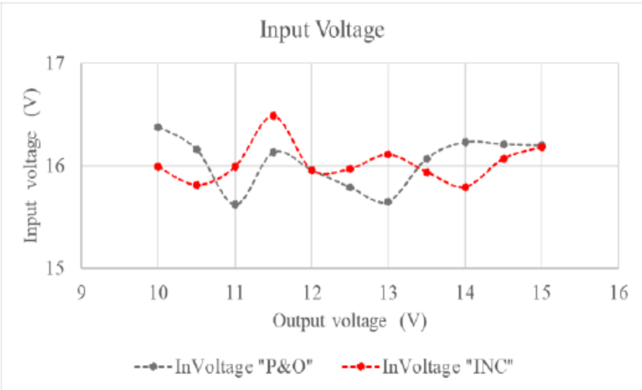


**Fig. 17: Input voltage with P&O and INC**

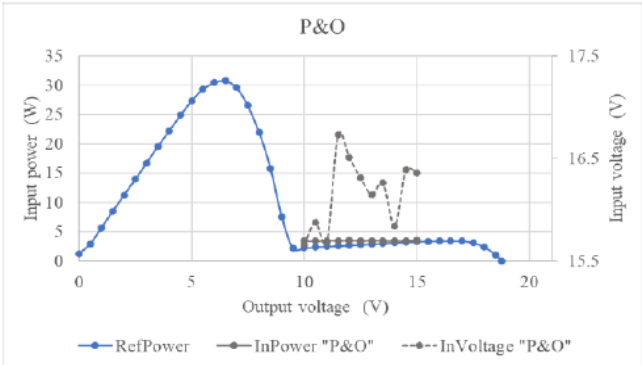


**Fig. 18: Input power and voltage with P&O**

**3. Total vertical shading**

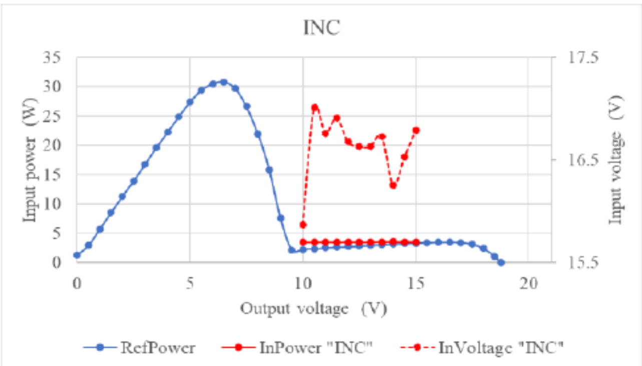


**Fig. 19: Input power and voltage with INC**

*Retrieval Number: 100.1/ijrte.A76260512123*
*DOI: 10.35940/ijrte.A7626.0512123*
*Journal Website: www.ijrte.org*



*Published By:*
*Blue Eyes Intelligence Engineering*
*and Sciences Publication (BEIESP)*

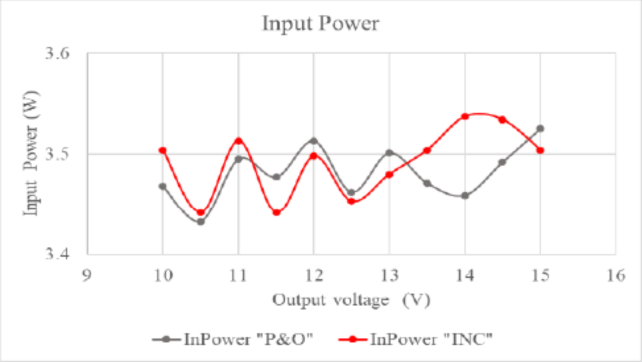


**Fig. 20: Input power with P&O and INC**

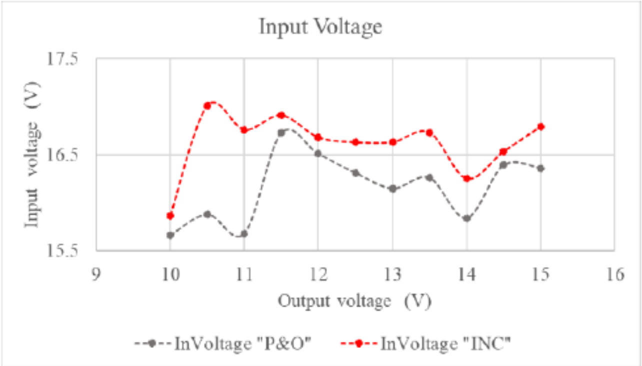


**Fig. 21: Input voltage with P&O and INC**

### B. Discussion

In full sunlight, for the first test, the PV module connected directly to the DC electronic load reaches a power peak around 70W for a Vmpp voltage of 14 to 15V (Fig. 10, Fig. 11, Fig. 12).

With the buck converter driven by the two commands P&O and INC, we have two cases on this first test:

- For an output voltage of 10 to 14V, in Fig. 13, the power at the input of the buck converter oscillates around the power peak for both controls.

The input voltage of the buck converter oscillates in the MPP zone with the INC command, which is not the case for the P&O command (it oscillates at the limit of this MPP zone).

- For an output voltage of 14 to 15V, in Fig. 13, a decrease in power and an increase in voltage at the input of the buck converter are observed for both controls.

This increase in the voltage at the input of the buck converter is explained by the voltage drop $\Delta V$ between the input and the output of the latter. On the order of 0.9V, this voltage drop $\Delta V$ is equal to the sum of the voltages at the terminals of (i) the shunt resistor R, (ii) the power MOSFET S1, (iii) the ESR of the inductor L, (iv) the blocking diode D2 and (v) the assembly of the "high-side" conductor of the buck converter (cf. Fig. 4).

From where its expression:

$$\Delta V = V_R + V_{S1} + V_L + V_{D2} + V_{HS}, \quad (12)$$

Therefore, in Fig. 13, when the output voltage is equal to that of the MPP zone, the input voltage cannot equal the output voltage because of this voltage drop which forces it to increase (to go out of the Vmpp voltage range) and to lose power.

For the second test, the PV module connected directly to the DC electronic load reaches a power peak around 2W for a Vmpp voltage of 15.5 to 16.5V (Fig. 14, Fig. 15, Fig. 16).

With both P&O and INC controls in Fig. 17, for an output voltage of 10 to 15V, the buck converter input power oscillates around the power peak and the input voltage is inside the MPP range.

The Vmpp voltage range is always higher than the output voltage, so both controls have a margin to drive the buck converter input voltage to reach the maximum power.

For the last test, the PV module connected directly to the DC electronic load reaches a power peak around 3.5W for a Vmpp voltage of 15 to 17V (Fig. 18, Fig. 19, Fig. 20).

Like the second test, the input power to the buck converter oscillates around the reference peak and the input voltage is inside the MPP region, regardless of the output voltage with both controls (Fig. 21).

## IV. CONCLUSION

The objective of this paper is to compare with laboratory tests the performance of the P&O and INC controls driving a buck converter, with different PV module conditions and a variable output voltage using a DC electronic load (from 10 to 15V, with a step of 0.5V every 5s). The power supplied by a PV module connected directly to a DC electronic load is selected as the object of comparison.

The equipments used are (i) a 100W PV module SPP031001200 manufactured by Victron energy, a synchronous buck converter driven by an Atmel ATmega V-2560 arduino board having a frequency of 31.25 kHz and a programmable DC electronic load of type 72- 13210 manufactured by TENMA™.

The P&O and INC performed well for a $V_{mpp}$ voltage range above the buck converter output voltage. However, they fail to stabilize the PV module power around the peak as soon as the buck converter output voltage is equal to the $V_{mpp}$ voltage range. This power loss is explained by the voltage drop $\Delta V$ between the input and output voltages of the buck converter, which forces the input voltage out of the Vmpp voltage range.

For a PV module exposed to full sunlight, the INC method performs better than the P&O method. For a PV module exposed to a horizontal or vertical total shading, the INC method gives a small advantage compared to the P&O method, which can be beneficial for a long time.

The choice of 10-15V buck converter output voltage aims to show the performance of the MPPT control for a 12V battery in charge mode. A MPPT type solar charge controller uses MPPT control during the bulk phase where the battery voltage is typically below a threshold voltage of 14.4V or 28.8V depending on the installation voltage and the battery technology.

It should be noted that all tests were carried out without considering the irradiance and the temperature due to the lack of measuring instruments.

*Retrieval Number: 100.1/ijrte.A76260512123*
*DOI: 10.35940/ijrte.A7626.0512123*
*Journal Website: www.ijrte.org*



*Published By:*
*Blue Eyes Intelligence Engineering*
*and Sciences Publication (BEIESP)*

## DECLARATION


| | |
|---|---|
| Funding/ Grants/ Financial Support | No, I did not receive. |
| Conflicts of Interest/ Competing Interests | No conflicts of interest to the best of our knowledge. |
| Ethical Approval and Consent to Participate | No, the article does not require ethical approval and consent to participate with evidence. |
| Availability of Data and Material/ Data Access Statement | Not relevant. |
| Authors Contributions | All authors have equal participation in this article. |


## REFERENCES


1. M. Boillot, A. Doulet, and N. Saincy, Electrification latérale : Vers un nouveau modèle d'électrification pour l'Afrique, Paris : Fondation Tuck, 2018.
2. M. Rebecca and E. Ergen, Le secteur de l'énergie en Afrique subsaharienne : état des lieux et perspectives, La Revue de l'Energie no. 626, 2015.
3. WWF, Diagnostic du secteur énergie à Madagascar, Rapport Septembre 2012.
4. A. Voninirina and S. Andriambelosoa, *Étude sur l'énergie à Madagascar*, Centre de recherches, d'études et d'appui à l'analyse économique à Madagascar, 2014.
5. Étienne Beeker, 2017/2027 - Energie centralisée ou décentralisée ? – Actions critiques, France Stratégie, 2017
6. A. Wheldon, C. Sharma, and E. Dobbs, 15 ans d'initiatives dans l'accès à l'électricité renouvelable décentralisée : l'expérience des Ashden Awards, Field Actions Science Reports, Paris, 2016.
7. A. Georgelin, Le secteur de l'énergie à Madagascar : Enjeux et opportunités d'affaires, 2016.
8. L. Richard, C. Boudinet, A. S. S. Ranaivoson, J. O. Rabarivao, A. E. Befeno, D. Frey, M. C. Alvarez-Hérault, B. Raison, N. Saincy, "Development of a DC Microgrid with Decentralized Production and Storage: From the Lab to Field Deployment in Rural Africa," *Energies MDPI*, vol. 15, no. 18, 6727, 2022. [CrossRef]
9. L. Richard, D. Frey, M. C. Alvarez-Hérault, B. Raison, "Experimental Design of Solar DC Microgrid for the Rural Electrification of Africa," *Proceedings of the PCIM Europe, Nurnberg, Germany*, pp. 1–10, 2022.
10. A. S. S. Ranaivoson, N. Le Saux, N. Saincy, E. J. R. Sambatra, T. Andrianajaina, T. D. Razafimahefa, "Comparison of two MPPT controls in a nanogrid. *International Journal of Education and Research*," vol.10, no. 9, pp. 143 – 158, 2022.
11. M. Scott, "A switched extremum seeking approach to maximum power point tracking in photovoltaic systems," *Grid Integration of Alternative Energy Sources*, Berkeley, 2009.
12. S. S. Ahmad and H. M. Y. Abdul, "Dynamic evolution control for synchronous buck DC–DC converter: Theory, model and simulation," *Simulation Modelling Practice and Theory, Elsevier*, vol. 18, no. 5, pp. 663-676, 2010. [CrossRef]
13. A. Rufer and P. Barrade, Cours d'électronique de puissance – Conversion DC/DC, Masson, 1994.
14. H. Abbes, H. Abid, K. Loukil, A. Toumi, and M. Abid, "Etude comparative de cinq algorithmes de commande MPPT pour un système photovoltaïque," *Revue des Energies Renouvelables*, vol. 17, no. 3, pp. 435-445, 2014
15. S. Li, "A MPPT control strategy with a variable weather parameter and no DC/DC converter for photovoltaic systems," *Solar Energy*, vol. 108, pp. 117-125, 2014 [CrossRef]
16. H. Rezk, A. M. Eltamaly, "A comprehensive comparison of different MPPT techniques for photovoltaic systems," *Solar Energy*, vol. 112, pp. 1-11, 2015. [CrossRef]
17. N. Aouchiche, M. S. Aït Cheikh, A. Malek, "Poursuite du point de puissance maximale d'un système photovoltaïque par les méthodes de l'incrémentation de conductance et la perturbation & observation," *Revue des Energies Renouvelables*, vol. 16, no. 3, pp. 485-498, 2013.
18. M. Saad, A. El Hammoumi, and A. El Ghzizal, "Photovoltaic systems with quantitative comparative between an improved MPPT and existing INC and P&O methods under fast varying of solar irradiation," *Energy Reports*, vol. 4, pp. 341-350, 2018. [CrossRef]


## AUTHORS PROFILE

**Sandaniaina Sedinirina Andriamihaingo Ranaivoson** received his Engineer's degree in Electrical Engineering from Higher Polytechnic School of Antsiranana in 2017. His research interests include Photovoltaic Systems, DC-DC converter, MPPT control, and smart grid.

**Nicolas Saincy** is a Co-founder of Nanoé - Decentralized electrification, who is a company whose objective is to develop access to electricity and employment in Africa by relying on renewable energies, local entrepreneurship and information and communication technologies.

**Eric Jean Roy Sambatra** has a Ph.D. degree in Electrical engineering. He is currently teaching at School of Industrial Engineering, Higher Institute of Technology of Antsiranana. His research interest is in the areas of Renewable energy systems, Electrical machines, Photovoltaic Systems, Wind turbines, Rural electrification, and NGD design engineering.

**Todizara Andrianajaina** has a Ph.D. degree in science and technology. He is currently teaching at Higher Polytechnic School of Antsiranana. His research interest is in the areas of Electrical & Electronics Engineering, Photovoltaic Systems, Fault Detection, Renewable Energy Technologies.

**Nirinason Jean Razafinjaka** is currently teaching as a Professor at Higher Polytechnic School of Antsiranana. His research interest is in the areas of Power Factor Correction, Control Theory, Automation & Robotics, Automotive Engineering, Artificial Neural Networks, Fuzzy Logic Control, Automation, Systems Dynamics, Control and Instrumentation, Optimal Estimation.